

A Diagnostic Method for Induction Motor Inter-Turn Faults Based on Wavelet Transform and Neural Networks

Diwakar Verma^{1,2*}, Dr. Ambarisha Mishra³

¹Research Scholar, Department of Electrical Engineering, NIT Patna, India.; Email: diwakarvermasonu@gmail.com

²Assistant Professor, EE Department, Bhagalpur College of Engineering, Bhagalpur; Email: diwakarvermasonu@gmail.com

³Assistant Professor, EE department, NIT Patna, Bihar, India; Email: ambrish.mishra@nitp.ac.in

*Correspondence: Email: diwakarvermasonu@gmail.com; Tel.: +91-7870763953

ABSTRACT- Conventional protection systems for induction motors often fail to detect inter-turn short circuit (ITSC) faults accurately. These faults are usually misclassified as overload or phase imbalance, which may lead to unnecessary tripping and downtime. Early detection of ITSC faults is important, as fault severity increases rapidly due to insulation degradation. This paper presents a diagnostic method based on wavelet transform and artificial neural networks (WTANN). The method uses stator current signals for fault detection without requiring additional sensors. The extracted features are used to classify motor conditions as ITSC, overload (OL), or short circuit fault (SCF). Experimental results on a 1 Hp, 415 V induction motor show that the proposed method achieves 97.4% testing accuracy, compared to 24.44% for the FFT-based method. The method performs well even under noisy conditions (20 dB and 30 dB). The results show that the proposed approach is accurate and suitable for practical applications.

Keywords: Induction Motor, Protection, Inter-Turn Fault, Wavelet Transform, ANN.

ARTICLE INFORMATION

Author(s): Diwakar Verma, and Dr. Ambarisha Mishra;

Received: 27/01/26; **Accepted:** 02/05/26; **Published:** 25/06/26;

E- ISSN: 2347-470X;

Paper Id: IJEER 2701B09;

Citation: 10.37391/ijeer.140222

Webpage-link:

<https://ijeer.forexjournal.co.in/archive/volume-14/ijeer-140222.html>

Publisher's Note: FOREX Publication stays neutral with regard to jurisdictional claims in Published maps and institutional affiliations.



1. INTRODUCTION

Three-phase induction motors (IMs) with low power ratings are widely used in applications such as cooling, ventilation, and pumping. These motors are common in power plants and industrial systems. IMs below 60 HP account for about 88% of winding failures [1], while higher-rated IMs contribute only 12%. This shows that low-power motors are more exposed to failure. Early detection of stator inter-turn short-circuit (ITSC) faults is very important for safe and reliable operation of IMs. These faults mainly occur due to insulation degradation. The insulation weakens because of electrical, thermal, mechanical, or environmental stress. As a result, small defects are formed inside the winding creating local hot spots, which further damage the insulation. ITSC faults disturb the balance of three-phase currents. This leads to higher losses, increased heating, vibrations, and rotor eccentricity. If the fault is not detected early, it can become severe. This may result in major failures such as winding damage, fire, or even explosion.

Industries that use critical equipment need reliable fault detection systems. These systems should detect small faults at an early stage. For this purpose, sensitive online monitoring

techniques are required. Early detection of ITSC helps in reducing downtime, maintenance cost, and improves system reliability. However, the challenge lies in developing non-invasive, cost-effective solutions that can be applied across various industrial sectors without compromising the system's sensitivity or accuracy. However, to effectively detect stator inter-turn short-circuits (ITSCs) and reduce failure rates, small and low-power induction motors (IMs) require cost-efficient techniques. Developing these solutions is critical for ensuring reliable operation while maintaining affordability, particularly in applications where expensive detection systems or continuous monitoring are impractical.

The main goal of fault diagnosis techniques is to identify winding problems by analyzing the frequency of the supply winding current. For precise parameter identification in induction machines, the technique suggested in [2] makes use of stator current loci; yet, this method did not address ITSC flaws. By examining three-dimensional waveforms of three-phase currents, the authors of [3] were able to identify stator ITSC problems. Although motor current signature analysis (MCSA) and vibration analysis are popular methods for fault diagnosis, they sometimes have trouble distinguishing between low-severity defects. Therefore, to improve fault detection, hybrid methods are preferred over single-signal techniques. These methods use more than one type of signal or mathematical analysis. In [5], vibration signals were combined with the wavelet transform for fault detection. In [4], a support vector machine was used with total harmonic distortion of stator voltage and current to identify defects. In [6], machine learning models were combined with both vibration and current data to improve condition monitoring and fault diagnosis. These approaches help increase detection accuracy and reliability.

Recent research has moved toward using advanced signal processing and artificial intelligence (AI) to detect stator faults more accurately and at an earlier stage. A neural fuzzy adaptive method was introduced in [7] to identify inter-turn faults in single-phase induction motors, while [9] applied artificial neural networks (ANNs) to analyze and classify stator fault conditions. A broader comparison of AI-based classifiers was carried out in [8], and a dedicated fault detection network targeting early-stage stator faults was proposed in [10]. Further efforts have focused on combining AI with well-established diagnostic methods. The work in [11] integrated neural networks with motor current signature analysis (MCSA) to improve detection reliability, and [12] implemented a CRIO-based real-time monitoring system for stator fault identification. These approaches generally report high classification accuracy under tested conditions. However, a common limitation across AI-based methods is their dependence on the quality and diversity of training data. As pointed out in [13], when the operating conditions during testing differ from those used during training — such as variations in load, speed, or supply voltage — the model's performance can degrade noticeably. This remains a practical concern when deploying these systems in real industrial environments where operating conditions are rarely constant.

Apart from the methods discussed above, other machine learning techniques such as Extreme Learning Machine (ELM), Convolutional Neural Networks (CNN), and Long Short-Term Memory (LSTM) networks have also been explored for fault classification in [23] and [24], each having its own set of limitations. ELM is a relatively straightforward feedforward neural network with a single hidden layer. While it offers faster training compared to deeper networks, this simplicity comes at the cost of classification accuracy, making it less suitable for fault detection tasks that require fine discrimination between operating conditions [23]. CNN, by contrast, is a far more computationally demanding approach. Before classification can take place, the raw time-series current signals must first be converted into the frequency domain and then further transformed into a two-dimensional image format known as a scalogram. This multi-step preprocessing pipeline adds considerable complexity to the overall system and places heavy demands on processor memory, making CNN-based solutions difficult to justify economically for low-cost motor protection applications [24]. LSTM networks, which are generally well-regarded for handling sequential and time-series data, also fall short when applied to ITSC fault classification. The core difficulty is that the differences in frequency component magnitudes between healthy and faulty motor conditions are very small. LSTM networks struggle to resolve these subtle distinctions reliably, which leads to misclassification — particularly in early-stage or low-severity fault scenarios.

Monitoring stray flux within the air gap is generally more practical for high-power induction motors, given the costs and invasiveness associated with these measurements. The authors of [15] recommended using internal flux measurement for the detection of inter-turn defects, whereas [14] suggested an

invasive observer coil-based technique for measuring total harmonic distortion (THD) in induced voltages. Additionally, transient analysis of stray flux was employed by [16] to assess fault conditions. By measuring stray flux at multiple sites, the authors of [17] and [18] examined Park's flux vector calculation and suggested integrating infrared and Hall effect sensors to improve temperature and flux measurement for inter-turn fault detection. The Wing Technique, created by [19], does not take stator problems into account but uses symmetrical components to diagnose rotor flaws. Negative sequence component-based methods offer another avenue for inter-turn fault detection, as any asymmetry introduced by an ITSC fault will naturally manifest in the negative sequence current. However, these methods have a well-known practical weakness — the negative sequence component is not exclusive to fault conditions. Supply voltage unbalances, load variations, and small asymmetries that exist in the winding structure even under healthy conditions all contribute to the negative sequence signal in a similar way. This makes it difficult to confidently attribute an observed negative sequence component to an actual fault rather than to normal operating irregularities. Further limitation is that negative sequence components, on their own, carry limited information about where in the machine the fault has occurred. Identifying which specific phase is affected requires additional analysis beyond what the negative sequence signal alone can provide, adding complexity to the diagnostic process and reducing the overall practicality of these methods in straightforward industrial applications.

From the literature, it is observed that many methods require additional sensors or involve high computational complexity. Some methods also show reduced performance under varying operating conditions. To overcome these issues, this work proposes a simple and efficient WTANN-based method using only stator current signals.

A comprehensive online system has been devised to diagnose ITSC problems in IMs using only the supply currents, taking into account the severity of faults and the crucial constraints of existing methods. The data collecting system is used to obtain the three-phase currents. For each cycle, the peak value of each phase current is first determined. A phase is marked for additional examination if it shows a peak larger than one per unit (pu). This approach effectively reduces the computational burden on the relay processor. Finally, discrete wavelet transform is applied to the identified signals, and the processed data is classified using ANN. Thus, the original contributions of this paper are as follows:

- The method uses only stator current, so no extra sensors are needed.
- A simple peak current check (>1 pu) is used to reduce unnecessary calculations.
- Only three important features (F1–F3) are selected to reduce complexity.
- The method works well even with noise (20 dB and 30 dB).
- It can clearly distinguish between ITSC, OL, and SCF faults

The rest of the paper is organized as follows: in *section 2* mathematical modeling of IM under normal and ITSC fault is analyzed. In *section 3*, the WTANN algorithm is described in detail while, in *section 4*, the experimental setup used along with its results is discussed in detail. And finally, the paper ends with concluding remarks.

2. MATHEMATICAL MODELING OF IM UNDER ITSC

Figure 1 illustrates a 3-phase IM experiencing ITSC fault on phase A of stator winding. The number of short-circuited turns is indicated by n_{sa2} , whereas the number of healthy turns is indicated by n_{sa1} . α , which is the ratio of the number of shorted turns to the total number of turns in the phase winding, provides the proportion of shorted turns given by eq. (1).

$$\alpha = \frac{n_{sa2}}{(n_{sa2} + n_{sa1})} \quad (1)$$

The parameter α represents the severity of the fault. A higher value of α means more turns are shorted, which indicates a more severe fault condition. αR_s and αL_{ls} are the short-circuited turns resistance and leakage reactance, respectively, where R_s refers to the stator winding's per-phase resistance, and L_{ls} represents its per-phase leakage inductance. The circulating short-circuits current if is measured, and it is assumed that the external fault impedance, symbolized by R_{sf} , is resistive in nature. The dynamics of IM having magnetically coupled rotor and stator is given by eq. (2) [14]

$$\begin{aligned} \bar{v}_{sabc} &= \frac{d}{dt} \lambda_{sabc} + R_s \bar{i}_{sabc} \\ 0 &= \frac{d}{dt} \lambda_{rabc} + R_{rabc} \bar{i}_{rabc} \end{aligned} \quad (2)$$

Where, i , v , R , and λ are the current, voltage, resistance and flux linkage of IM. The variables used in the subscript *i.e.* a , b , and c represent the phases while, s and r stand for the stator and rotor. This equation represents the electrical behavior of the induction motor. It shows the relationship between voltage, current, and flux linkages in both stator and rotor circuits. The representation of three-phase voltages, currents, and flux linkages is represented by eq. (3). Also, the developed electromagnetic torque of IM under ITSC fault is expressed by eq. (4) where, θ_r stands for rotor position and P is the number of poles.

$$\begin{aligned} \bar{v}_{sabc} &= \begin{bmatrix} \bar{v}_{sa1} \\ \bar{v}_{sa2} \\ \bar{v}_{sb} \\ \bar{v}_{sc} \end{bmatrix}, \bar{i}_{sabc} = \begin{bmatrix} \bar{i}_{sa} \\ (\bar{i}_{sa} - \bar{i}_f) \\ \bar{i}_{sb} \\ \bar{i}_{sc} \end{bmatrix} \\ \bar{i}_{rabc} &= [\bar{i}_{ra} \quad \bar{i}_{rb} \quad \bar{i}_{rc}]^T \\ \lambda_{sabc} &= \begin{bmatrix} \lambda_{sa1} \\ \lambda_{sa2} \\ \lambda_{sb} \\ \lambda_{sc} \end{bmatrix} = L_{ss} \bar{i}_{sabc} + L_{sr} \bar{i}_{rabc} \\ \lambda_{rabc} &= \begin{bmatrix} \lambda_{ra} \\ \lambda_{rb} \\ \lambda_{rc} \end{bmatrix} = L_{sr}^T \bar{i}_{sabc} + L_{rr} \bar{i}_{rabc} \end{aligned} \quad (3)$$

$$T_{ITSC} = \bar{i}_{sabc}^T \frac{dL_{sr}}{d\theta_r} \bar{i}_{rabc} \quad (4)$$

The flux linkage equations describe how the stator and rotor are magnetically coupled. The electromagnetic torque depends on this coupling and changes when a fault occurs.

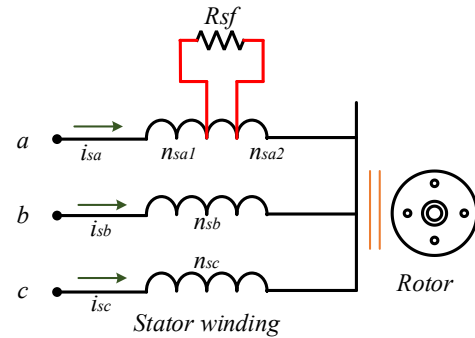


Figure 1. Squirrel cage induction motor with inter-turn short circuit fault on phase A

When an ITSC fault occurs in an IM, the overall equivalent impedance of the affected phase decreases, causing an increase in the phase current, as indicated by equation (5). As the fault progresses and more turns of the winding are affected, the phase current continues to rise. Additionally, the mutual inductances between phases are altered, leading to slight variations in the magnitude of the currents in the healthy phases. Although these deviations are smaller than those in the faulty phase, an imbalance among the phase currents is evident. This imbalance is used as a key indicator in the presented technique for further fault analysis.

$$|Z_{sf}| < |Z_a|, |\bar{I}_{af}| < |\bar{I}_a| \quad (5)$$

When an ITSC fault occurs, the impedance of the affected phase decreases. This leads to an increase in current in that phase. This change in current is used as the main indicator for fault detection in the proposed method. From the above analysis, it is clear that ITSC faults cause an increase and imbalance in phase currents. These changes are used in this work for feature extraction and fault classification.

3. PRESENTED WAVELET TRANSFORMS BASED ARTIFICIAL NEURAL NETWORK TECHNIQUE (WTANN)

The projected algorithm in this paper is designed to distinguish ITSC in IM by analyzing the signatures of the three-phase current. The algorithm is initialized when the peak current in any phase increases more than 1pu. Whenever any phase current *i.e.* i_{sx} ($x = a, b, c$) is greater than 1pu, then the next step is initiated. To extract different statistical features from the current signals that are recorded using a digital oscilloscope and sampled at a fixed rate, it makes use of the discrete wavelet transform (DWT). The current signal is broken down into several degrees of information and approximation using DWT. Both high- frequency and low-frequency components are captured by these deconstructed levels, which are crucial

for locating the ITSC issue. Features are extracted from the approximation as well as detail coefficients obtained from the wavelet decomposition and are combined into a feature vector that is fed into a three-layered feed forward neural network. The neural network can classify the state in which the motor is functioning; specifically, whether it is operating under normal conditions or whether a particular type of fault is occurring such as the inter-turn short circuit fault (ITSC), overload (OL), or short circuit fault (SCF). The use of feature vectors instead of raw signal data greatly decreases the computation power required for the classification process, making the methodology much more practical in terms of implementation. Moreover, the proposed method exhibits resilience with respect to changes in the electrical parameters, including the fault resistance as well as changes in load. The aim of this research is the development of a classification algorithm able to recognize several different types of faults in induction motors in order to increase the life cycle of the motor.

3.1. Discrete Wavelet Transform

The Discrete Wavelet Transform (DWT) is used to analyze signals at different frequencies. It can capture both high-frequency and low-frequency components of a signal. Unlike the Fourier Transform, which works only in the frequency domain, DWT works in both time and frequency domains. DWT divides the signal into two parts: approximation and detail. The approximation part contains low-frequency components. The detail part contains high-frequency components. This separation is done using low-pass and high-pass filters. The signal is decomposed step by step using these filters. The process of decomposition is shown in *figure 2*. In this work, DWT is used to analyze stator current signals. Since ITSC faults produce small and time-varying changes, DWT helps in capturing these variations effectively. This makes it more suitable than traditional FFT methods.

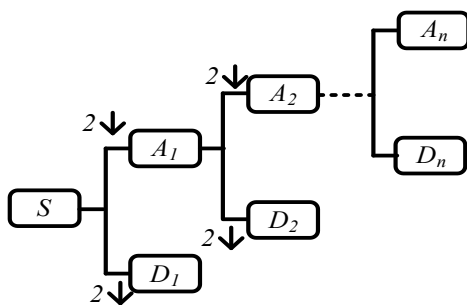


Figure 2. Decomposition of a signal with down sampling using DWT

- At each level of decomposition, the original signal $x[n]$ is passed through two filters—a low-pass filter $h[n]$ and a high-pass filter $g[n]$. These filters separate the signal into its approximation and detail components, respectively. The approximation and detail coefficients, which correspond to the low and high frequency content of the signal, are expressed by *eq. (6)* where, $A_j[n]$ and $D_j[n]$ denote the approximation and detail coefficients at the j^{th} level.
- Following the filtering process, the signal is down-sampled by retaining every second data point. This process reduces

the signal length and focuses on the relevant frequency components given by *eq. (7)*. By performing down-sampling, computational efficiency is achieved, allowing the DWT to operate effectively on large datasets.

- The process of filtering and down-sampling is applied iteratively to the approximation coefficients, resulting in a multi-level decomposition of the original signal. At each level, the signal is further divided to extract finer details. The main low-frequency part remains unchanged. This step-by-step process helps in capturing both small changes and overall trends in the signal.

$$A_j[n] = \sum_k x[k] h[2n - k]$$

$$D_j[n] = \sum_k x[k] g[2n - k]$$
(6)

$$A_j[n] = A_j[2n], D_j[n] = D_j[2n]$$
(7)

- The original signal can be reconstructed using the Inverse Discrete Wavelet Transform (IDWT). In this process, the approximation and detail coefficients are first up sampled. Then, they are passed through synthesis filters to rebuild the signal. The reconstruction equation is given in *eq. (8)*.

$$x[n] = \sum_k A_j[k] h[2n - k]$$

$$+ D_j[k] g[2n - k]$$
(8)

3.2. Feature Extraction and its selection

Before classification, a feature extraction technique is used to lower the dimensionality of the coefficients derived after the DWT. Since the db9 wavelet function performs well for electrical signals, it is used in this paper to compute the wavelet coefficients at various decomposition levels [21]. Before performing the decomposition, the signals are normalized to a p.u. value of one. Once the decomposition is complete, various statistical parameters are computed from the wavelet coefficients to extract meaningful features.

Only a portion of the retrieved features are chosen utilizing a correlation analysis method in order to further refine the feature collection. This method successfully removes extraneous characteristics that don't significantly relate to the event of interest. Measures including standard deviation, mean, kurtosis, energy, skewness, and root mean square (RMS) are among the statistical parameters that were chosen. Only those factors that offer pertinent information for classification are kept after these are assessed for every decomposition level. Only the statistically significant parameters are chosen for further classification tasks by using the correlation matrix approach to determine the most efficient collection of features.

The DWT is used in this investigation to break down the signal into five levels. Since the three-phase IM's fundamental

frequency is 50 Hz, a sampling frequency of 5 kHz is used to record the differences between events. The RMS value of level D_1 , the peak value of level A_3 , and the mean of level D_5 are chosen for additional examination among the characteristics that were retrieved using DWT. These characteristics, as stated in eq. (9), offer crucial details for categorizing IM dynamics under different faults.

$$\left. \begin{aligned} F_1 &= RMS(D_1) = \sqrt{\frac{1}{N-1} \sum_{n=1}^{N-1} x^2(n)} \\ F_2 &= Peak(A_3) = \max |x(n)| \\ F_3 &= Mean(D_5) = \frac{1}{N-1} \sum_{n=1}^{N-1} x(n) \end{aligned} \right\} \quad (9)$$

The selected features (F_1 , F_2 , and F_3) represent important characteristics of the signal such as energy, peak value, and average behavior. These features show clear separation between different fault conditions, which makes them suitable for classification. A boxplot of the feature F_1 , which illustrates its effectiveness in classifying various events in the IM, is displayed in figure 3. Though comparable boxplots were generated to evaluate the performance of each extracted feature set, only the results for F_1 is presented in this paper.

The remaining boxplots, although useful, have been excluded for shortness. Features with large variations and fewer outliers provide better classification performance. Therefore, only stable and consistent features are selected for further analysis.

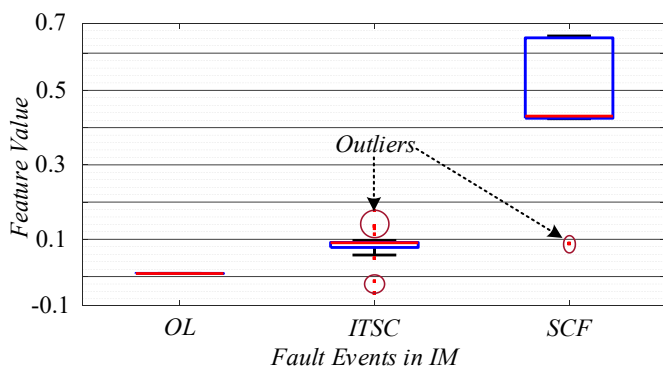


Figure 3. Boxplot of feature F_1 indicating its classification capability

By displaying important statistical points including the highest value, minimum value, first quartile (ψ_1), median (ψ_2), and third quartile (ψ_3), the boxplot offers a succinct overview of the dataset distribution. The method also detects outliers in the data. Outliers are values that are very different from the rest of the data. These points may lead to wrong classification. As shown in Figure 4, features with many outliers are removed from further analysis. This helps improve the accuracy of the method. By removing such unreliable features, the method

focuses on stable and consistent data. This improves overall classification performance. Figure 3 and figure 4 show the effectiveness of the selected features. In figure 3, overload (OL), ITSC, and short circuit fault (SCF) have clear and separate value ranges. These values are normalized in per unit (p.u.). In figure 4, the feature values are closely grouped. This makes classification difficult. To solve this problem, a boxplot method is used. It helps to clearly separate the feature distributions and improves classification accuracy.

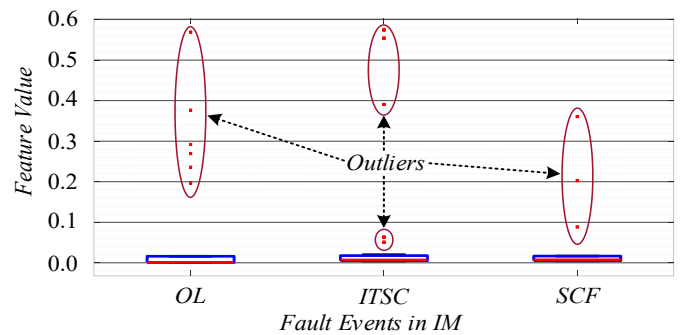


Figure 4. Boxplot of feature not included for further analysis as it is not having accurate classification accuracy

The neural network is trained using predefined weights and biases. A momentum constant and a learning rate are also set. The performance of the proposed method is evaluated offline using MATLAB. Different operating conditions are considered during training and testing. These include ITSC, short circuit fault (SCF), and overload (OL). About 80% of the data is used for training. The remaining 20% is used for testing and accuracy evaluation. To check the robustness of the method, noise is added to the data. Gaussian white noise is used for this purpose. Two signal-to-noise ratio (SNR) levels are considered: 20 dB and 30 dB. This helps evaluate the performance of the algorithm under different noise conditions. The results show that the method maintains good accuracy even in noisy environments. The steps of the proposed

WTANN method are given below:

- Acquire three-phase stator current signals.
- Normalize the signals in per unit (p.u.).
- Check the peak value of each phase current.
- If the current exceeds 1 p.u., that phase is selected for analysis.
- Apply discrete wavelet transform (DWT) to the selected signal.
- Extract features (F_1 , F_2 , F_3) from wavelet coefficients.
- Select important features using correlation and boxplot analysis.
- Feed the selected features to the ANN.
- Classify the motor condition as ITSC, OL, or SCF.

4. EXPERIMENTAL SETUP AND RESULTS

This study focuses on the effectiveness of the presented WTANN method in detecting stator ITSCs through an experimental setup involving a 4-pole, 1 Hp, 415 V, 50 Hz, 1.8A rated three-phase squirrel cage IM. The detailed

specifications of the motor are shown in *table 1*. *Figure 5* illustrates the block diagram of the system, while *figure 6* presents the laboratory prototype of IM having provision of windings to be shorted for the generation of ITSC. The setup includes a squirrel cage IM, a variable rheostat with a rating of 0.8Ω and 10 A, a resistive load bank, a three-phase variac, a mechanism for creating inter-turn faults, a digital oscilloscope (DSO) and a computer with MATLAB software. Additionally, current probes are employed to measure all three phase currents. The fault analysis unit receives voltage and current data from the DSO into the computer for further processing.

Table 1. Specifications of Laboratory Prototype Squirrel Cage IM

| Parameter | Rating |
|---------------|----------|
| Power | 1 hp |
| Voltage | 440V |
| Current rated | 1.8A |
| Frequency | 50Hz |
| Speed (Rated) | 1500 rpm |
| P_f | 0.83 lag |

| | |
|-----------------|--------|
| Turns of stator | 346/ph |
| Pole pair | 4 pole |

The ANN used in this work is a feedforward neural network with three input nodes, one hidden layer, and three output nodes. The input layer receives the selected features (F_1-F_3). The hidden layer processes the inputs using a sigmoid activation function. The output layer classifies the motor condition into ITSC, OL, or SCF. The network is trained using the backpropagation algorithm with a suitable learning rate and momentum constant. The training process continues until the error is minimized. A suitable learning rate and momentum constant are selected to ensure stable convergence. The activation function used in the hidden layer is sigmoid. The network is trained for multiple epochs until the error is minimized. The extracted features are used as inputs to the hidden layers of the network. The ANN is trained using the given dataset. After training, the network classifies the motor condition as ITSC, OL, or SCF. About 80% of the data is used for training. The remaining 20% is used for testing and validation. This helps in evaluating the performance of the network.

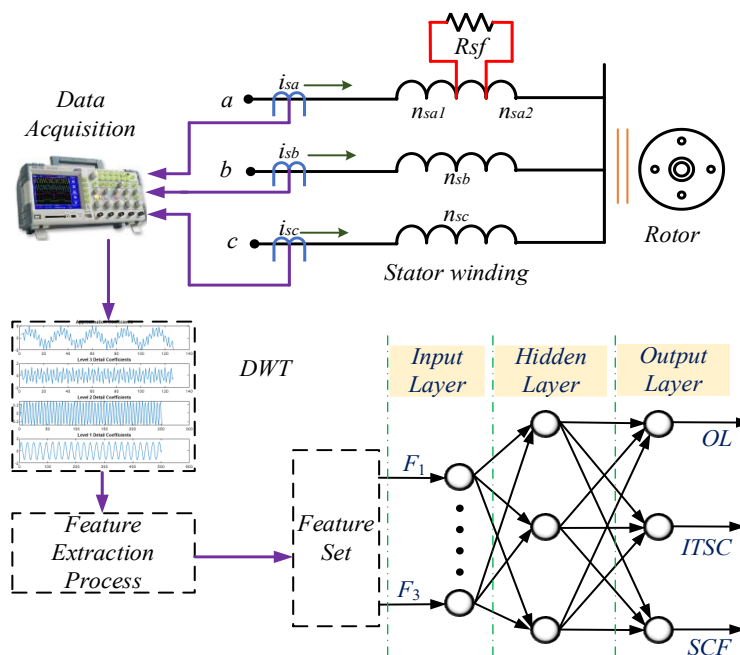


Figure 5. Block diagram of the presented algorithm

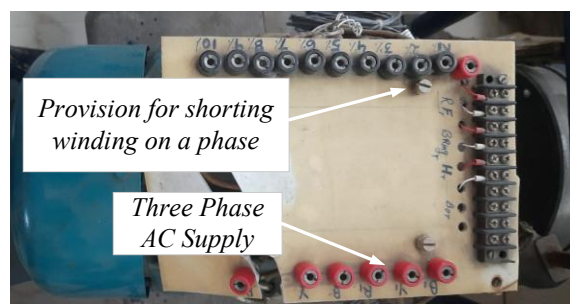


Figure 6. Laboratory prototype of squirrel cage IM with a provision for shorting turns

Data was collected at different motor speeds and different levels of shorted turns. A laboratory prototype was used to create controlled faults. The winding was shorted from 1% to 10% in small steps. The motor load was also varied from 0% to 100% in steps of 25%. For each shorting level, data was recorded for every cycle. Each measurement included three cycles of data. A total of 150 samples were collected for ITSC fault conditions. The experimental setup is shown in *figure 7*.

In addition to ITSC faults, an external fault was also created at the stator terminals. This was done using a rheostat to simulate different fault resistances. This condition produced high currents in all phases. Another 150 samples were collected for short circuit fault (SCF) conditions. Overload (OL) conditions were also tested. The motor load was increased from 100% to 120% of its rated value. This produced another 150 samples. Overall, the dataset includes ITSC, SCF, and OL conditions. This dataset is used for fault detection and classification.

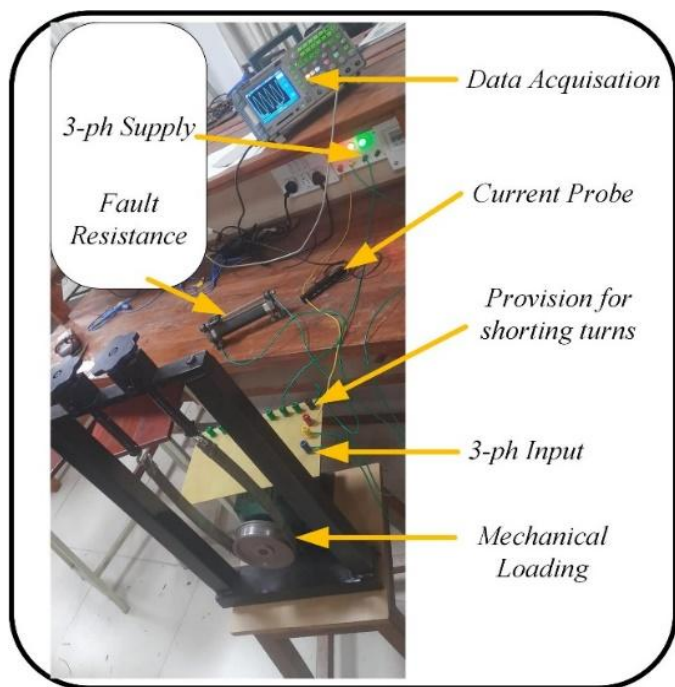


Figure 7. Experimental setup

To evaluate the performance of the proposed algorithm, Gaussian white noise was added to the data. Two noise levels were used: 20 dB and 30 dB. In total, 1,350 data samples were generated ($150 \times 3 \times 3 = 1350$). Out of these, 80% of the data (1,080 samples) was used for training the neural network. The remaining 20% (270 samples) was used for testing. This division helps in properly evaluating the performance and accuracy of the algorithm. This division of data allows for a robust evaluation of the algorithm's performance under various noise conditions and operational scenarios. The stator current under 20db noise and 2% ITSC condition is shown in *Figure 8*. The distortion in the waveform indicates the presence of fault. Also, the stator current of phase a with 4% shorting turns and 30db noise is shown in *figure 9*. The data is collected using a single-phase current probe by keeping the reference

point constant as shown in *figure 10*. The dataset includes different fault conditions, load variations, and noise levels. This ensures that the proposed method is tested under realistic operating conditions. The inclusion of noise at 20 dB and 30 dB helps in evaluating the robustness of the algorithm.

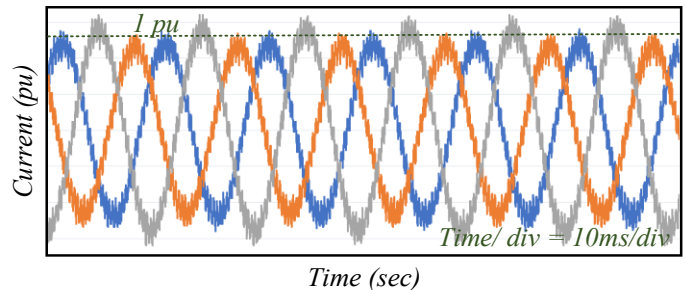


Figure 8. Stator current waveform under 2% ITSC fault with 20 dB noise

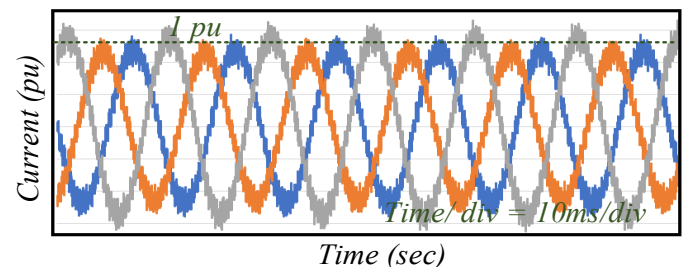
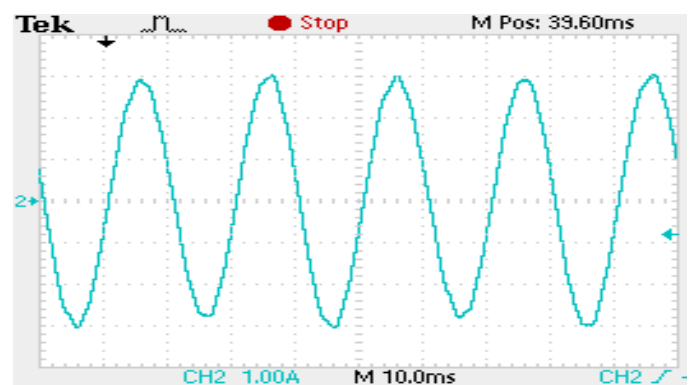


Figure 9. Stator current with 3% ITSC and 30db noise

The collected data is tested offline using MATLAB software. The samples that have been collected using DSO and sampled at 5 kHz are used to extract the features F_1 to F_3 using DWT which decomposed the current signal into 5 levels as mentioned earlier. These features are stored in a memory of MATLAB and are used for further evaluations. The featured data is randomly split into a ratio of 4:1 out of which 80% is fed to ANN for classification. The training results of ANN after an exhaustive iterative process is shown in *Table 2*. Where the performance of the presented algorithm is compared with the traditional Fast Fourier Transform (FFT) method which gives the total harmonic distortion (THD). The presented algorithm which is trained with multiple feature sets provides a training accuracy of 99.44% while the traditional technique only provides 38.79% accuracy.



(a)

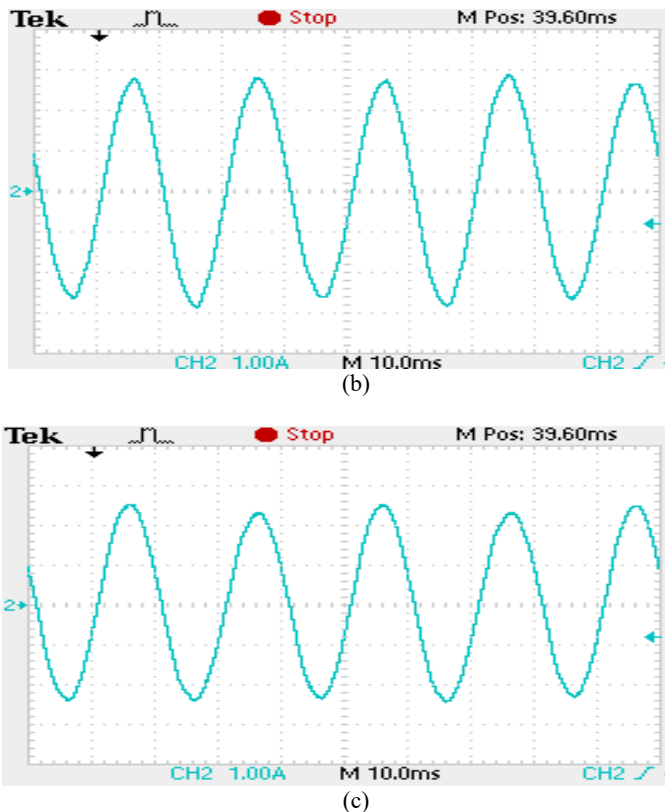


Figure 10. Phase currents during ITSC fault with same reference point of capture (a) R phase, (b) Y Phase, and (c) B Phase

while the traditional technique fails with 66 accurate classifications. The testing accuracy of the presented technique is 97.4% while the traditional technique has a lower accuracy of 24.44%. The accuracy for the presented algorithm while testing dropped from 99.44% to 97.40% since an additional gaussian white noise was added in the original signals.

Table 3. Testing results of ANN using DWT and FFT

| Condition / Training Data Set | | Classifier | |
|-------------------------------|-----|------------------------|-----------|
| | | DWT (F_1 to F_3) | FFT (THD) |
| <i>ITSC</i> | 90 | 87 | 21 |
| <i>SCF</i> | 90 | 88 | 15 |
| <i>OL</i> | 90 | 88 | 30 |
| Total | 270 | 263 | 66 |
| % Accuracy | | 97.40% | 24.44% |

From table 3, it can be observed that the proposed method maintains high accuracy even in the presence of noise. The small reduction in accuracy (from 99.44% to 97.4%) is due to the added Gaussian noise. However, the method still performs reliably. This shows that the proposed approach is robust and suitable for real-time applications. The testing results confirm that the proposed method maintains high accuracy even when noise is present. This shows that the method is robust and can work reliably under practical conditions. The proposed method is tested under different operating conditions to ensure reliable performance. These include variation in fault severity (1% to 10% shorted turns), load conditions (0% to 120%), and noise levels (20 dB and 30 dB). This wide range of conditions helps in validating the method for real industrial applications.

The FFT-based method provides only frequency-domain information and is not suitable for analyzing non-stationary signals. In contrast, DWT provides time-frequency analysis, which helps in capturing small and transient changes caused by ITSC faults. This is the main reason for the improved performance of the proposed WTANN method. The selected features (F_1 - F_3) show clear separation between fault conditions. This reduces overlap between classes and improves classification accuracy. At the same time, using only three features reduces computational complexity.

5. CONCLUSIONS

In conclusion, this paper presents a WTANN method in detecting ITSC and other fault conditions in a 3-ph squirrel cage IM. The custom-built laboratory prototype enabled the controlled simulation of faults, including ITSC, SCF, and OL conditions, across varying motor speeds, load levels, and shorted turns. A total of 1,350 samples were collected from different fault conditions, noise levels, and operating loads. This dataset is used to evaluate the proposed algorithm. The WTANN method uses features (F_1 to F_3) obtained from DWT for fault classification. It shows much better performance than the traditional FFT-based method. During training, WTANN achieved an accuracy of 99.44%. In comparison, the FFT method achieved only 38.79%. During testing, WTANN maintained high accuracy of 97.4%, even with added Gaussian

Table 2. Training results of ANN using DWT and FFT

| Condition / Training Data Set | | Classifier | |
|-------------------------------|------|------------------------|-----------|
| | | DWT (F_1 to F_3) | FFT (THD) |
| <i>ITSC</i> | 360 | 359 | 210 |
| <i>SCF</i> | 360 | 357 | 124 |
| <i>OL</i> | 360 | 358 | 85 |
| Total | 1080 | 1074 | 419 |
| % Accuracy | | 99.44% | 38.79% |

From table 2, it is clear that the proposed WTANN method performs significantly better than the FFT-based method. The higher accuracy of WTANN is due to the use of time-frequency analysis, which captures both transient and steady-state signal characteristics. In contrast, FFT only provides frequency-domain information and fails to capture non-stationary behavior. The high training accuracy of the WTANN method shows that the selected features are effective in representing fault conditions. The use of DWT allows the extraction of both high-frequency and low-frequency components, which improves feature quality compared to FFT.

To further evaluate the effectiveness of the presented algorithm, the remaining 20% data is tested for both traditional technique and the presented technique. The result of training data is shown in table 3 where out of 270 total signals 263 have been accurately classified by the presented algorithm

white noise (20 dB and 30 dB). The FFT method performed poorly, with an accuracy of only 24.44%. The main advantage of WTANN is its ability to analyze signals at different levels using DWT. This helps in capturing small changes and non-stationary behavior in fault conditions. The FFT method cannot capture these details effectively. WTANN is also robust to noise and can clearly distinguish between ITSC, SCF, and OL conditions. It works well under different operating and noise conditions. These results show that the proposed method is reliable and suitable for real industrial applications. It can be useful for predictive maintenance by reducing downtime and improving machine life.

Author Contributions: Conceptualization, D.V. and A.M.; methodology, D.V.; software, D.V.; validation, D.V. and A.M.; formal analysis, D.V.; investigation, D.V.; resources, A.M.; data curation, D.V.; writing—original draft preparation, D.V.; writing—review and editing, D.V. and A.M.; visualization, D.V.; supervision, A.M.; project administration, A.M.; funding acquisition, A.M. All authors have read and agreed to the published version of the manuscript.

Funding Source: “This research received no external funding”

Conflicts of Interest: “The authors declare no conflict of interest.”

REFERENCES

- [1] Athikessavan Subash Chandar, Elango Jeyasankar, Panda Sanjib Kumar. Inter-turn fault detection of induction motors using end-shield leakage fluxes. *IEEE Trans Energy Convers* 2022. <http://dx.doi.org/10.1109/TEC.2022.3174891>.
- [2] Reed David M, Hofmann Heath F, Sun Jing. Offline identification of induction machine parameters with core loss estimation using the stator current locus. *IEEE Trans Energy Convers* 2016;31(4):1549–58.
- [3] Eftekhari Maryam, Moallem Mehdi, Sadri Saeed, Hsieh Min-Fu. Online detection of induction motor’s stator winding short-circuit faults. *IEEE Syst J* 2013;8(4):1272–82.
- [4] Singh Girish Kumar, Ahmed Saleh Al Kazzaz Sa’ad. Vibration signal analysis using wavelet transform for isolation and identification of electrical faults in induction machine. *Electr Power Syst Res* 2004;68(2):119–36.
- [5] Patel Rakesh A, Bhalja Bhavesh R. Condition monitoring and fault diagnosis of induction motor using support vector machine. *Electr Power Compon Syst* 2016;44(6):683–92.
- [6] Ali Mohammad Zawad, Shabbir MdNasmus SakibKhan, Liang Xiaodong, Zhang Yu, Hu Ting. Machine learning-based fault diagnosis for single-and multi-faults in induction motors using measured stator currents and vibration signals. *IEEE Trans Ind Appl* 2019;55(3):2378–91.
- [7] Ballal Makarand S, Khan Zafar J, Suryawanshi Hiralal M, Sonolikar Ram L. Adaptive neural fuzzy inference system for the detection of inter-turn insulation and bearing wear faults in induction motor. *IEEE Trans Ind Electron* 2007;54(1):250–8.
- [8] Palácios Rodrigo H Cunha, Silva Ivan Nunes Da, Goedtel Alessandro, Godoy Wagner F. A comprehensive evaluation of intelligent classifiers for fault identification in three-phase induction motors. *Electr Power Syst Res* 2015;127:249–58.
- [9] Bazan Gustavo Henrique, Scalassara Paulo Rogério, Endo Wagner, Goedtel Alessandro, Godoy Wagner Fontes, Palácios Rodrigo Henrique Cunha. Stator fault analysis of three-phase induction motors using information measures and artificial neural networks. *Electr Power Syst Res* 2017;143:347–56.
- [10] Husari Fatimatelbatoul, Seshadrinath Jeevanand. Early stator fault detection and condition identification in induction motor using novel deep network. *IEEE Trans Artif Intell* 2021. <http://dx.doi.org/10.1109/TAI.2021.3135799>.
- [11] Mejia-Barron Arturo, Tapia-Tinoco Guillermo, Razo-Hernandez Jose R, Valtierra-Rodriguez Martin, Granados-Lieberman David. A neural network-based model for MCSA of inter-turn short-circuit faults in induction motors and its power hardware in the loop simulation. *Comput Electr Eng* 2021;93. <http://dx.doi.org/10.1016/j.compeleceng.2021.107234>.
- [12] Sarkar Shubhashish, Purkait Prithwiraj, Das Santanu. NI Compact RIO-based methodology for online detection of stator winding inter-turn insulation faults in 3-phase induction motors. *Measurement* 2021;182. <http://dx.doi.org/10.1016/j.measurement.2021.109682>.
- [13] Gangsar Purushottam, Tiwari Rajiv. Signal based condition monitoring techniques for fault detection and diagnosis of induction motors: A state-of-the-art review. *Mech Syst Signal Process* 2020;144:106908.
- [14] Surya Gulamfaruk N, Khan Zafar J, Ballal Makarand S, Suryawanshi Hiralal M. A simplified frequency-domain detection of stator turn fault in squirrel-cage induction motors using an observer coil technique. *IEEE Trans Ind Electron* 2016;64(2):1495–506.
- [15] Mirzaeva Galina, Saad Khalid Imtiaz. Advanced diagnosis of stator turn-to-turn faults and static eccentricity in induction motors based on internal flux measurement. *IEEE Trans Ind Appl* 2018;54(4):3961–70.
- [16] Ramirez-Nunez Juan A, Antonino-Daviu Jose A, Climente-Alarcón Vicente, Quijano-López Alfredo, Razik Hubert, OsornioRios Roque A, Romero-Troncoso Rene de J. Evaluation of the detectability of electromechanical faults in induction motors via transient analysis of the stray flux. *IEEE Trans Ind Appl* 2018;54(5):4324–32.
- [17] Gyftakis Konstantinos N, Marques Cardoso Antonio J. Reliable detection of stator interturn faults of very low severity level in induction motors. *IEEE Trans Ind Electron* 2020;68(4):3475–84.
- [18] Kumar Padmanabhan Sampath, Xie Lihua, Halick Mohamed Sathik Mohamed, Vaiyapuri Viswanathan. Stator end-winding thermal and magnetic sensor arrays for online stator inter-turn fault detection. *IEEE Sens J* 2020;21(4):5312–21.
- [19] Dongare Ujwala Vikas, Umre Bhimrao Sitaram, Ballal Makarand Sudhakar. Rotor winding inter-turn short-circuit fault detection in wound rotor induction motors using Wing Technique. *J Power Electron* 2022;22(4):614–28.
- [20] P. C. Krause, O. Wasynczuk, and S. D. Sudhoff, *Analysis of Electric Machinery and Drive Systems*, 2nd ed., IEEE Press, 2002.
- [21] Kamble, S.P., Thawkar, S., Gaikwad, V.G. et al. A Comparative Analysis for Selection of Appropriate Mother Wavelet for Detection of Stationary Disturbances. *J. Inst. Eng. India Ser. B* 98, 533–540 (2017).
- [22] Kamble, S., Chaturvedi, P., Chen, C.J. et al. Enhancing reliability and efficiency of grid-connected solid-state transformer through fault detection and classification using wavelet transform and artificial neural network. *Electr Eng* 106, 2525–2535 (2024). <https://doi.org/10.1007/s00202-023-02080-2>.
- [23] Ratna, S., Muflih, M., Budiman, H., Syapoto, U., & Hamdani, M. (2024). Comparison of ELM, LSTM, and CNN Models in Breast Cancer Classification. *Journal of Data Science*, 2024.
- [24] Adnan Dehghani, Hamza Mohammad Zakir Hiyat Moazam, Fatemehsadat Mortazavizadeh, Vahid Ranjbar, Majid Mirzaei, Saber Mortezaei, Jing Lin Ng, Amin Dehghani, Comparative evaluation of LSTM, CNN, and ConvLSTM for hourly short-term streamflow forecasting using deep learning approaches, *Ecological Informatics*, Volume 75, 2023, 102119.



© 2026 by Diwakar Verma, and Dr. Ambarisha Mishra. Submitted for possible open access publication under the terms and conditions of the Creative Commons Attribution (CC BY) license (<http://creativecommons.org/licenses/by/4.0/>).